

BIOLOGICAL AND PHYTOCHEMICAL INVESTIGATION OF *DAPHNE MUCRONATA* WITH SPECIAL EMPHASIS ON GCMS AND EDX ANALYSIS.

Nadia Faqir^{1*}, Soha Ali¹, Hafiza Saima Zafar¹, Sayed Farhan Ali², Sadam Hussain², Noreen Khan³, Hassan Raza Javeed⁴

¹Department of Botany, Islamia College Peshawar, KP, Pakistan.

²Department of Biotechnology, Abdul Wali Khan University Mardan, KP, Pakistan.

³Department of Botany, University of Peshawar, KP, Pakistan.

⁴Department of Botany, Government Graduate College Layyah, Punjab, Pakistan.

*Corresponding author: nadiafaqir321@gmail.com

Submission Date: 21/03/2024

Acceptance: 31/03/2024

Online: 07/04/2024

Abstract: The study current investigated the extracts of *D. mucronata* for their comprehensive biological and phytochemical potential. Antibacterial study revealed that *Klebsiella pneumonia*, *Clavibacter michiganensis* showed 30% inhibition to Ethylacetate and chloroform extract at the same concentration of 18 μ l. least activity was shown by *Clavibacter michiganensis* at concentration 6 μ L. The present antifungal investigation declared that highest inhibition was 28.5% and 29%, examined by *C. albicans* at concentrations 12 μ L by n-hexane and aqueous 18 μ l fractions, least activity was also shown by *C. albicans* 17.5% at 6 μ L in chloroform extraction. Furthermore, the phytotoxic study revealed that *D. mucronata* extracts had inhibitory effects on the growth of *Daucus carrota* and *Brassica campestris*, with higher concentrations leading to more pronounced inhibition of plumule and radicle lengths in both plant species. Finally, the GC-MS analysis identified several compounds in the chloroform extracts of *D. mucronata*, including camphor, caryophyllene oxide, ar-tumerone, thujanone, terpinen-4-ol, hexahydrofarnesyl acetone, cyclohexyl methane, trans-1,2-dimethylcyclohexane, 2,2,3,4-Tetramethylpentane, and 2,3,3-Trimethyloctane. Additionally, the EDX analysis revealed the elemental composition of *D. mucronata*, with carbon and oxygen being the major elements, along with trace amounts of magnesium, silicon, phosphorus, sulfur, chlorine, potassium, and calcium. In summary, this comprehensive study sheds light on the bioactive properties of different fractions of *D. mucronata*, providing valuable understandings into its potential pharmaceutical and agricultural applications.

Index-terms: *D. mucronata*, Antibacterial, Antifungal, Phytotoxic, GCMS, and EDX.

I. INTRODUCTION

Phytochemistry serves as an essential basis for the validation of a wide range of therapeutic enterprises, the discovery of crude pharmaceuticals, and the achievement of a beneficial anthropological action (Mukherjee et al., 2015). There have been many ways to figure out the physical and chemical composition of different chemicals. Gas Chromatography-Mass Spectroscopy (GC-MS) is used to look at the extracts to figure out how much active ingredient there is in herbs used in cosmetics, drugs, pharmaceuticals, food, the environment, and forensics. A single method called "analytical" can be used to look at mixtures of chemical compounds. It separates the different parts of the mixture, and mass spectroscopy looks at each one separately to figure out chemical compounds based on mass spectra (Naron et al., 2017). Energy Dispersive X-

Ray Spectroscopy (EDX) analysis is a method to analyze a sample, determine its composition or appearance and how the sample interacts with the X-ray source. The fundamental premise of spectroscopy is that each element's electromagnetic emission spectrum has a distinct collection of peaks due to its unique atomic structure (Kara et al., 2020). According to Arndt et al. (2016), one effective method for determining the size, shape, and structure of individual particles is energy dispersive X-ray spectrometry, more often known as EDX analysis. The benefits of innate antibacterial elements include developed consistency, a reduced risk of spinoff, and harmful consequences. In order to treat infectious infections, which are unavoidable, we need to produce antifungal treatments that are resistant to the antifungal drugs that are already available, either via natural resistance or through the development of resistance (Pinto et al., 2017). According to Imatomi et al. (2015), Phytotoxicity has emerged as a crucial tool for identifying plants that contain bioactive substances. These plants may then be used in the creation of natural herbicides that are more specific and result in fewer environmental compensations. Health care services have been put in jeopardy during the last several years as a result of the widespread use of antibiotics that are less effective against a variety of infections (Bhalodia and Shukla, 2011).

Daphne mucronata has high hopes for traditional medicine because of its many bioactive components, which include coumarins, flavonoids, and triterpenoids. Few studies have examined its distribution patterns and how it reacts to environmental changes, despite the fact that it is an evergreen shrub with a long history of medical use and ecological significance (Ashraf et al., 2018). From its antioxidant and antibacterial capabilities to its potential in treating a wide range of illnesses and conditions, including cancer and skin disorders (Zaidi et al., 2015), this article compiles what is known about the medicinal characteristics of *D. mucronata*. It also highlights the need for more research and preservation initiatives by illuminating the dynamics of this plant species' global dispersal, especially in areas like Iran and Pakistan. The article emphasizes the importance of *D. mucronata* as a valuable resource for both traditional medicine and potential pharmaceutical applications. It takes a multidisciplinary approach, encompassing ethnobotanical, phytochemical, and pharmacological studies. The potential therapeutic benefits of *D. mucronata* has been focused through current targeted research.

II. MATERIALS AND METHODS

2.1 Identification, Gathering, and Preservation

The plant *D. mucronata* was gathered in Swat KPK, a distinct district of Pakistan. The Plant was Identified based on characteristics and literature with eflora and the identification was confirmed by Dr. Naveed Akhtar (Taxonomist) Department of Botany, Islamia College Peshawar. The stem, leaves, and flowers of the *D. mucronata* were first washed before being air dried at room temperature. The powder from the plant was saved in a plastic bag for later usage after all of the dried pieces were ground in an electronic grinder with a 12000 rpm speed.

2.2 Crude Extract Preparation

Following the method of (Lutfullah et al., 2019) The stem, leaves, and shoots were prepared for grinding after the samples had fully dried. The 1000ml of methanol was combined with 1000g of the ground herbal powder. The mixes are kept on a

shaker at lab temperature for three days. Using Whatman's filter paper, the aforementioned combinations were filtered to eliminate solid material, and a clean filtrate was produced. The filtered extract was then moved to a rotary evaporator where it was vacuum-distilled to eliminate the solvents and ultimately produce a potent extract.

2.3 Fractionation

As per (Imran et al., 2021) with the aid of an isolating funnel, the crude extract was re-dissolved in 100 ml of water and fractionated using various natural solvents, including water, ethanol, chloroform, and n-hexane. The filtrate's fluid composition then switched to the isolating funnel that had been 3:1 boosted with n-hexane. The substance in the funnel began to vigorously shake after that, and it continued to do so for a while as it was left to collect specific amounts of aqueous and n-hexane. In the isolating channel, n-hexane, which has a lower molecular weight than water, remained as a layer on top. N-hexane was left behind in the funnel layer after the first layer of water, which was collected in a separate glass container, was added. The N-hexane layer is then transferred to another glass beaker. With the aid of an isolating funnel, the crude extract was dissolved in 100 ml of water and fractionated using various natural solvents, including water, ethylacetate, chloroform, and n-hexane. The fluid arrangement of the filtrate then switched to the isolating funnel that had been 3:1 augmented with n-hexane. The mixture within the funnel began to vigorously shake after then. It continued to shake for a while after that in order to achieve specific amounts of aqueous and n-hexane. N-hexane, which has a lower molecular weight than water, persisted as a layer on top in the isolating channel. N-hexane was left behind in the funnel layer after the first layer, which was composed of water collected in a separate glass container. Later, transfer the N-hexane layer to another glass beaker. In a similar fashion, the extra layer of distilled water was also subjected to fractionation using n-butanol and chloroform. In a rotary evaporator set to 40°C and 60 rpm, every fractionation part was evaporated. In a similar fashion, the extra layer of distilled water was also subjected to fractionation using n-butanol and chloroform. In a rotary evaporator set to 40°C and 60 rpm, every fractionation part was evaporated.

2.4 Antibacterial Activity

Following in Faden's footsteps, agar in a well diffusion was used to see bacteria anticipating and fighting against the concentrations (2018). Four distinct solvent plant extracts were used in the measurement.

2.4.1 Microorganisms Used

For antibacterial activity, five different bacterial strains *X. vesicatoria*, *Enterobacterial common antigen*, *Klebsella pneumonia*, *Clavibacter michiganensis*, and *E. carotovora* were used.

2.4.2 Inoculation Procedure

In order to examine a unique suspension of bacterial culture and assume that the total number of microorganisms is coupled as per MacFarland's standard, the McFarland principle [106 state framing unit] was used. Later, the broth was introduced to an inoculant.

2.4.3 Growth Medium for Bacteria

By thoroughly combining 500ml of distilled water with 20 grams of nutritional agar, media against bacterial activity was prepared, followed the footstep of (Karamolah et al., 2017). The media were placed in an autoclave for twenty minutes at

121°C and 15 psi pressure to purify them. Media were placed in a laminar stream hood for cooling after sterilization. The media were injected into each plate in an amount of 15 ml when the temperature fell below 40°C.

2.4.4 Gelatin Petri Dish Preparation

After distillation, the nutrient broth was poured into neat petri dishes and kept cool. The entire microbial colony was placed inside 15 milliliter centrifugation tubes with fixed caps. A sanitary drill was used to create small holes in the petri plates while sixty microliters of a twenty-four-hour combination of each inoculate was added.

2.4.5 Stock Solution Preparation

According to (Lutfullah et al., 2019) after rotating evaporation, the rough concentrates were dissolved in 10% DMSO at a ratio of 3 ml to every 36 mg. Fluconazole was used as the definitive control, while absolute DMSO was the negative control.

2.4.6 Inhibitory Zone of Growth and Measuring

Each well was filled with the use of a syringe and mixtures of varying concentration and paired capacity. Separate plates were used for the positive and negative controls, and they were placed in an incubator for 24 hours at a temperature of 37 °C. 24 hour success. The area affected by the areas that the decoction used caused obstructions was taken into consideration.

2.5 ANTIFUNGAL ACTIVITY

2.5.1 Parasitic Strain Utilized

The disease causing fungus *Aspergillus nigar*, *C. albicans* were picked up from the pathology department of Agriculture University of Peshawar. These species were then used for antifungal activity.

2.5.2 Media Preparation for Fungal Growth

Preparation of the media for fungus development PDA of 20 grams was dissolved in 500 ml of sterile water and sterilized for 20 minutes at 15 psi and 121°C to prepare the medium. Autoclaved media was placed within a laminar flow hood and allowed to cool there at ambient temperature. When the medium temperature dropped to 50°C, the sterilized media was put into sterilized petri dishes. Faden (2018) modified his approach to address the streaking of fungus on media. The studied fungus was made into a fresh culture by adding 1ml of cultured stock to 9ml of freshly produced PDA. This culture was used for incubation after 24 hours. In comparison to MacFarland's standard solution, the growth of this culture was visually assessed. Assuring the fungal development was spurted with a micropipette on the media top, then escalated using a streaker. Using a sterilized steel tool, holes were built around equal gaps after that, and media was removed using clean tongs. Raw extract or its fractions were poured into these wells in three separate concentrations of 30, 60, and 90. In isolated plates, fluconazole was used as a positive control in three different concentrations, while fungus was the only factor in the negative control. Plates were paraffin-sealed to prevent contamination. These plates were incubated at 37 °C for 24 hours. The reading was obtained by constructing an X-Y axis and measuring the zone of inhibition. Three times for each fraction were used in the computation to get an exact answer, and the average and standard deviation were estimated after that.

2.6 Phytotoxic Activity

To check the phytotoxic effects on the selected plants seed powder was taken following (Fujii et al., 2004) with slight changes. 1-liter media was prepared as per standard method that is 15gm agar per 1 liter distilled water. Then it was put to autoclave to sterilize it. And was fold into petri dishes to solidify inside sterile ambins under laminar flow hood.

3 concentrations 10mg/20mg/30mg were selected and was added to the petri plates. Each petri plates were provided with 10 seeds of the two tests plants (*Daucus carrota* and *Brassica compestris*), and was kept at 24°C for 72 hours in dark.

2.7 GCMS Analysis

The Gas Chromatography-Mass Spectrometry (GC-MS) analysis was carried out with the assistance of a device that was outfitted with a mass spectrometer, a front injection source, and a GC inlet. Following a ramping program that reached 270 degrees Celsius at a rate of 10 degrees Celsius per minute and was maintained for thirteen minutes, the GC technique required a run duration of thirty-six minutes. The starting oven temperature was set at seventy degrees Celsius for three minutes. Equilibration time was set at 2 minutes, with a maximum temperature of 300°C. The injection was performed using a 10 µL syringe, delivering 1 µL of the sample. The injection system utilized solvent A and solvent B washes both pre and post-injection, each with 6 washes of 8 µL volume. Sample washes were carried out with 4 washes of 8 µL volume. The injection was dispensed at a speed of 6000 µL/min. The front injector operated in split mode with a split ratio of 20:1 and a split flow of 20 mL/min. The column used was a DB-1 with dimensions 30 m x 250 µm x 0.25 µm. Helium was used as the carrier gas. In the mass spectrometer, the acquisition mode was set to scan with a solvent delay of 2 minutes. The scan parameters included a start time of 2 minutes, scanning from 30 to 650 m/z, with a threshold of 150 and 4 A/D samples. The MS source temperature was set at a maximum of 250°C, and the MS quad temperature at a maximum of 200°C. Tune parameters were set for the instrument, with trace ion detection turned off. Various parameters such as emission, energy, ion focus, and entrance lens were optimized for efficient ionization and detection. The actual EM volts used were 1082.8, and the gain factor was set to 1.00. Mass gain and offset were also adjusted accordingly. The method provided a comprehensive approach for the analysis of samples using GC-MS, ensuring efficient separation and detection of compounds present in the sample matrix (Li et al., 2020).

2.8 Energy Dispersive X-ray (EDX) Analysis

The prepared powder samples of *D. mucronata* were taken to the Centralized Resource Laboratory (CRL) at the University of Peshawar for analysis. With the help of an energy dispersive X-ray (EDX-7000, Na-U, Shimadzu, Japan) and the loose powder method, the samples were measured and calibrated against an Al-Cu reference. Interior the EDX-7000 spectrometer is a one-gram powder from the samples that were put on the inside. The apparatus is equipped with an X-ray tube with a Rhodium (Rh) target and a high-performance silicon drift detector (SDD), which can run at a maximum of 50 KeV and 1000 A, as well as the PCEDX-Navi software for navigation. The elemental makeup of all samples was determined in an environment that was primarily composed of air. The analytes were then evaluated with a collimator with a diameter of 10 mm and a live acquisition period of the 60s using a 10 mm collimator (Khan et al., 2021).

III. RESULTS

3.1 ANTIBACTERIAL ACTIVITY

3.1.1 N-hexane Fraction

The antibacterial activity of the n-hexane fraction of *D. mucronata* was evaluated against several pathogenic bacterial strains, including *K. pneumonia* (*K. pneumonia*), *E. carotovora*, *X. vesicatoria*, and *Clavibacter michiganensis* (*C. michiganensis*). In the control group, where no n-hexane fraction was added, all four bacterial strains exhibited substantial growth with zone of inhibition values of 47.5 mm for *K. pneumonia*, 44 mm for *X. vesicatoria*, 47 mm for *C. michiganensis*, and 47 mm for *E. carotovora*. However, when the n-hexane fraction of *D. mucronata* was introduced at various concentrations (6 μ g/ml, 12 μ g/ml, and 18 μ g/ml), it showed significant antibacterial activity. At 6 μ g/ml, the zone of inhibition for *K. pneumonia* was reduced to 19.5 mm, while for *X. vesicatoria*, it was 15.5 mm. *C. michiganensis* and *E. carotovora* also exhibited decreased growth with inhibition zones of 16 mm and 15.5 mm, respectively. With an increase in concentration to 12 μ g/ml, the inhibitory effects were more pronounced. *K. pneumonia* displayed a zone of inhibition of 22 mm, *X. vesicatoria* showed 19.5 mm, *C. michiganensis* had 19 mm, and *E. carotovora* exhibited a zone of inhibition of 21.5 mm. At the highest concentration tested, 18 μ g/ml, the n-hexane fraction displayed the most potent antibacterial activity. *K. pneumonia* was inhibited with a zone size of 28.5 mm, *X. vesicatoria* had 27.5 mm, *C. michiganensis* showed 26.5 mm, and *E. carotovora* exhibited a remarkable zone of inhibition of 32 mm. These results indicate that the n-hexane fraction of *D. mucronata* possesses significant antibacterial properties, with its efficacy increasing with higher concentrations.

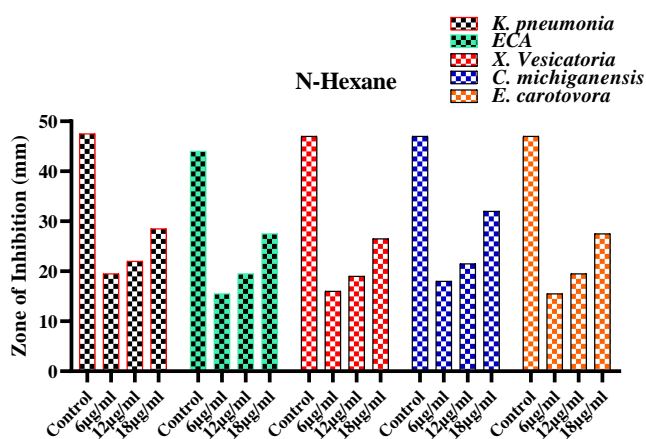


Fig. 3.1.1 The antibacterial effects of N-hexane fraction of *D. mucronata* against the given bacterial strains.

3.1.2 Chloroform Fraction

The antibacterial activity of *D. mucronata*'s chloroform fraction was evaluated against several bacterial strains, including *K. pneumonia* (*K. pneumonia*), *X. vesicatoria* (*X. vesicatoria*), *Clavibacter michiganensis* (*C. michiganensis*), and *E. carotovora* (*E. carotovora*). The results revealed that the chloroform fraction exhibited significant antibacterial potential against all the tested bacterial strains. At the highest tested concentration of 18 μ g/ml, the chloroform fraction demonstrated the most substantial inhibitory effects. It produced inhibition zones of 26mm against *K. pneumonia*, 24.5mm against *X. vesicatoria*, 35.5mm against *C. michiganensis*, and 24.5mm against *E. carotovora*. As the concentration of the chloroform

fraction decreased, the zone of inhibition generally decreased as well, which is expected in dose-dependent antibacterial activity. Even at the lowest concentration of 6 μ g/ml, the chloroform fraction still exhibited notable inhibitory effects against the tested bacterial strains, with inhibition zones ranging from 16mm to 18.5mm.

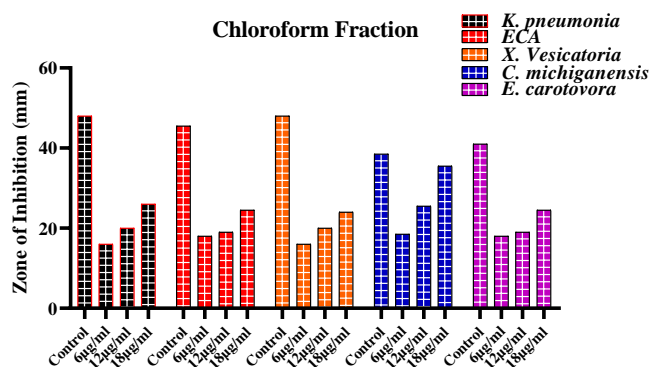


Fig. 3.1.2 The antibacterial effects of chloroform fraction of *D. mucronata* against the given bacterial strains.

3.1.3 Ethyl Acetate Fraction

The results of the antibacterial activity of the ethyl acetate (ECA) fraction from *D. mucronata* against various bacterial strains are presented in the table. The study investigated the inhibitory effects of different concentrations of the ECA fraction on four bacterial strains, namely *Klebsiella pneumonia*, *X. vesicatoria*, *Clavibacter michiganensis*, and *E. carotovora*. In the control group, where no ECA fraction was applied, the bacterial strains exhibited varying degrees of growth inhibition, with zone sizes ranging from 39.5 mm to 47.5 mm. This variability in susceptibility suggests differences in the sensitivity of the tested bacteria to natural compounds found in the ethyl acetate fraction. Upon treatment with the ECA fraction at concentrations of 6 μ g/ml, 12 μ g/ml, and 18 μ g/ml, distinct trends in antibacterial activity emerged. At the lowest concentration of 6 μ g/ml, the ECA fraction displayed moderate inhibitory effects, with zone sizes ranging from 18 mm to 21 mm. Notably, the ECA fraction exhibited the highest inhibitory activity against *E. carotovora* at this concentration, with a zone of inhibition measuring 21 mm. As the concentration of the ECA fraction increased to 12 μ g/ml and 18 μ g/ml, a significant enhancement in antibacterial activity was observed against all tested bacterial strains. The zone of inhibition expanded for each strain, indicating a dose-dependent response. The most notable increase in inhibition was observed against *Klebsiella pneumonia*, which showed a substantial growth inhibition zone of 33.5 mm at the highest concentration of 18 μ g/ml.

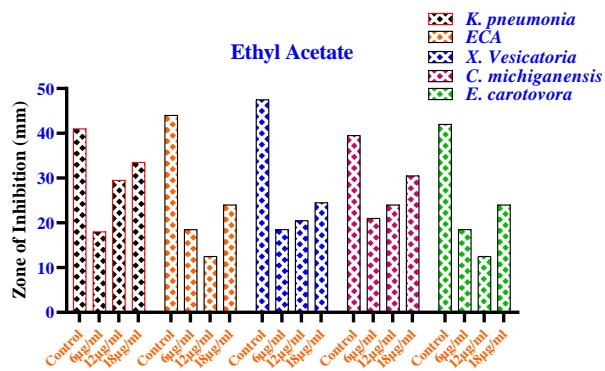


Fig. 3.1.3 The antibacterial effects of ethyl acetate fraction of *D. mucronata* against the given bacterial strains.

3.2 ANTIFUNGAL ACTIVITY

3.2.1 N-hexane Fraction

The antifungal activity of the N-hexane fraction of *D. mucronata* was evaluated against two common fungal pathogens, *C. albicans* and *A. Niger*. In the control group, where no N-hexane fraction was applied, the zone of inhibition for *C. albicans* was 29.5 mm, while it was 28 mm for *A. Niger*. As the concentration of the N-hexane fraction increased, a noticeable decrease in the zone of inhibition was observed for both fungi. At a concentration of 6µg/ml, the zone of inhibition for *C. albicans* decreased to 20 mm, and for *A. Niger*, it decreased to 23.5 mm. However, at higher concentrations of 12µg/ml and 18µg/ml, the antifungal activity seemed to improve for *C. albicans*, with zones of inhibition measuring 28.5 mm and 27.5 mm, respectively. In contrast, the antifungal activity against *A. Niger* remained relatively stable, with zones of inhibition of 22.5 mm and 25.5 mm at 12µg/ml and 18µg/ml, respectively.

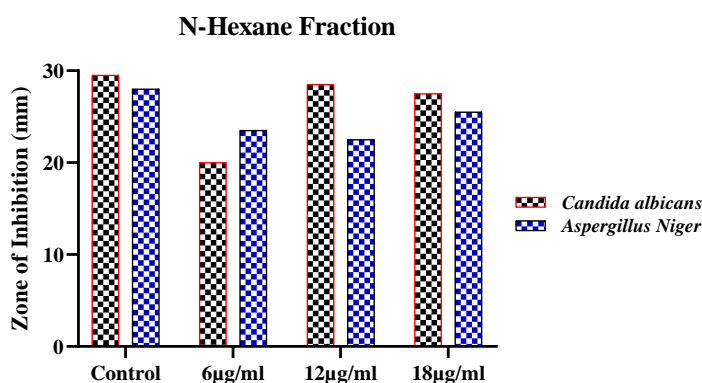


Fig. 3.2.1 The antifungal effects of N-hexane fraction of *D. mucronata* against the given fungal strains.

3.2.2 Chloroform Fraction

The antifungal activity of *D. mucronata* was assessed through the chloroform fraction, and the results revealed a significant impact on the growth of both *C. albicans* and *A. Niger*. In the control group, where no chloroform fraction was added, the zone of inhibition was 32.5 mm for *C. albicans* and 27 mm for *A. Niger*. However, when the chloroform fraction was

introduced at various concentrations, a dose-dependent response was observed. At 6 μ g/ml concentration, the zone of inhibition decreased to 17.5 mm for *C. albicans* and 18 mm for *A. Niger*. Increasing the concentration to 12 μ g/ml resulted in a slight improvement in antifungal activity, with zones of inhibition measuring 19.5 mm for *C. albicans* and 19 mm for *A. Niger*. The most substantial inhibitory effect was observed at 18 μ g/ml concentration, with a zone of inhibition of 20 mm for *C. albicans* and a notable increase to 24 mm for *A. Niger*.

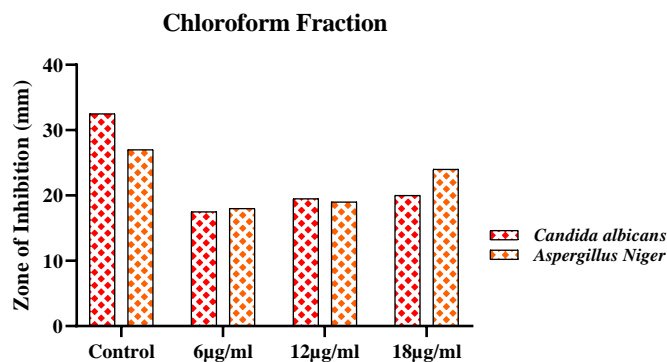


Fig. 3.2.2 The antifungal effects of chloroform fraction of *D. mucronata* against the given fungal strains.

3.2.3 Ethyl Acetate Fraction

The chloroform fraction of *D. mucronata* was evaluated for its antifungal activity against two common fungal pathogens, *C. albicans* and *A. Niger*. In the control group, where no fraction was added, the inhibition zone for *C. albicans* was measured at 30.5 mm, while for *A. Niger*, it was 25 mm. As the concentration of the chloroform fraction increased, a noticeable decrease in the zone of inhibition was observed for both fungal strains. At a concentration of 6 μ g/ml, the zone of inhibition for *C. albicans* was 23 mm, and for *A. Niger*, it was 19 mm. This trend continued as the concentration of the fraction increased to 12 μ g/ml, with inhibition zones of 23.5 mm for *C. albicans* and 18.5 mm for *A. Niger*. Surprisingly, at the highest tested concentration of 18 μ g/ml, the zone of inhibition for *C. albicans* decreased to 22.5 mm, but it increased to 22 mm for *A. Niger*.

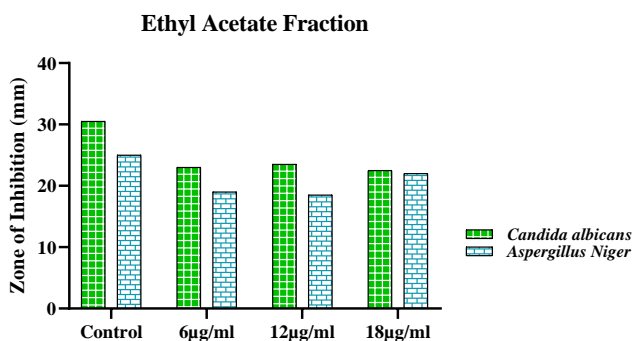


Fig. 3.2.3 The antifungal effects of ethyl acetate fraction of *D. mucronata* against the given fungal strains.

3.3 Phytotoxic Activity

The phytotoxic activity of *D. mucronata* extracts was evaluated against two commonly encountered plant species, *Daucus carrota* (carrot) and *Brassica campestris* (mustard). The experiment involved different concentrations of the extracts (10mg, 20mg, and 30mg) and a control group (100%). The effects of these extracts were assessed by measuring the length of plumule and radicle of both plant species.

For *D. carrota*, it was observed that the extracts exhibited varying degrees of phytotoxicity at different concentrations. At 10mg, the plumule length was 0.51 ± 0.63 mm, while the radicle length was 1.52 ± 1.38 mm. At 20mg, the plumule length slightly increased to 0.56 ± 0.69 mm, while the radicle length decreased to 1.36 ± 1.48 mm. The highest concentration tested, 30mg, resulted in a further reduction in plumule length to 0.32 ± 0.42 mm and radicle length to 1.12 ± 1.41 mm. In contrast, the control group exhibited significantly longer plumule and radicle lengths, with a plumule length of 0.91 ± 0.40 mm and a radicle length of 3.93 ± 0.62 mm (Fig. 3.3.1a).

Similarly, for *B. campestris*, the *D. mucronata* extracts showed phytotoxic effects. At 10mg, the plumule length was 0.91 ± 0.61 mm, and the radicle length was 3.01 ± 1.62 mm. At 20mg, the plumule length remained relatively consistent at 0.90 ± 0.81 mm, while the radicle length decreased to 2.9 ± 1.95 mm. The highest concentration of 30mg resulted in a further decrease in plumule length to 0.50 ± 0.72 mm and radicle length to 1.13 ± 1.39 mm. The control group, as expected, exhibited significantly longer plumule and radicle lengths, with a plumule length of 1.76 ± 0.76 mm and a radicle length of 4.22 ± 1.44 mm (Fig. 3.3.1b). In summary, the phytotoxic activity of *D. mucronata* extracts was evident in both plant species, with higher concentrations of the extracts leading to more pronounced inhibitory effects on plumule and radicle growth.

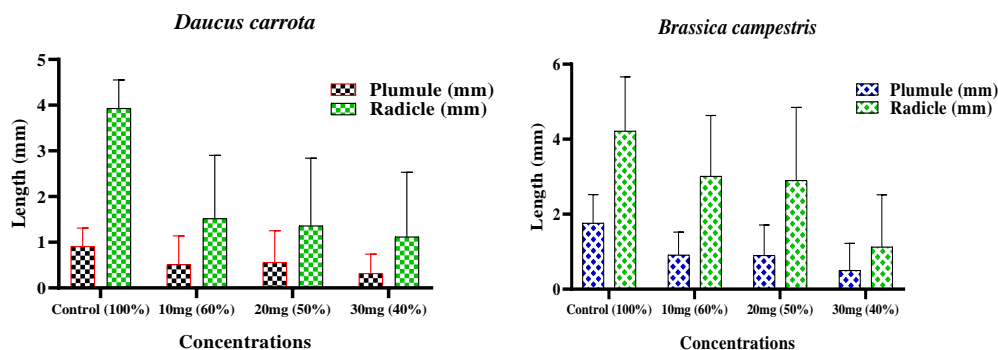


Fig. 3.3.1a & b. The phytotoxic activity of *D. mucronata* extracts different concentrations against *D. carrota* and *B. campestris*.

3.4 Gas Chromatography and Mass Spectrometry

The Gas Chromatography-Mass Spectrometry (GC-MS) analysis of chloroform extracts from *D. mucronata* revealed the presence of several compounds. Camphor ($C_{10}H_{16}O$, 152.23 g/mol), a bicyclic monoterpene, was identified as the first compound. Additionally, Caryophyllene oxide ($C_{15}H_{24}O$, 220.35 g/mol), an oxygenated sesquiterpene, was detected. Ar-tumerone ($C_{15}H_{20}O$, 216.32 g/mol), another sesquiterpene, was also identified. Thujanone ($C_{10}H_{16}O$, 152.23 g/mol), a compound with a molecular mass identical to camphor, was found. Terpinen-4-ol ($C_{10}H_{18}O$, 154.25 g/mol), a monoterpene alcohol, was detected as well. Hexahydrofarnesyl acetone ($C_{18}H_{36}O$, 268.5 g/mol), a sesquiterpene, was among the

compounds present. Cyclohexyl methane ($C_{27}H_{36}O_2$, 392.6 g/mol), a cycloalkane derivative, was also identified. Additionally, trans-1,2-dimethylcyclohexane (C_8H_{16} , 112.21 g/mol), 2,2,3,4-Tetramethylpentane (C_9H_{20} , 128.25 g/mol), and 2,3,3-Trimethyloctane ($C_{11}H_{24}$, 156.31 g/mol) were detected in the analysis.

Table 3.4.1 GCMS analysis and list of compounds found in chloroform extract of the *D. mucronata*.

S.No	Compound Name	Molecular Formula	Molecular Mass
1	Camphor	$C_{10}H_{16}O$	152.23g/mol
2	Caryophyllene oxide	$C_{15}H_{24}O$	220.35g/mol
3	Ar-tumerone	$C_{15}H_{20}O$	216.32g/mol
4	Thujanone	$C_{10}H_{16}O$	152.23g/mol
5	Terpinen-4-ol	$C_{10}H_{18}O$	154.25g/mol
6	Hexahydrofarnesyl acetone	$C_{18}H_{36}O$	268.5g/mol
7	Cyclohexyl methane	$C_{27}H_{36}O_2$	392.6g/mol
8	trans-1,2-dimethylcyclohexane	C_8H_{16}	112.21g/mol
9	2,2,3,4-Tetramethylpentane	C_9H_{20}	128.25g/mol
10	2,3,3-Trimethyloctane	$C_{11}H_{24}$	156.31 g/mol

3.5 Energy Dispersive X-Ray (EDX) Analysis

The results of the Energy-Dispersive X-ray (EDX) analysis of *D. mucronata* reveal the elemental composition of this botanical specimen. Carbon is the dominant element, constituting a significant 69.82% by weight and 76.47% by atomic percentage. Oxygen is also a major component, comprising 27.15% by weight and 22.32% by atomic percentage. In addition to these primary elements, trace amounts of other elements were detected, including magnesium (0.28% by weight, 0.15% by atomic percentage), silicon (0.23% by weight, 0.11% by atomic percentage), phosphorus (0.4% by weight, 0.17% by atomic percentage), sulfur (0.74% by weight, 0.3% by atomic percentage), chlorine (0.21% by weight, 0.08% by atomic percentage), potassium (1.03% by weight, 0.35% by atomic percentage), and calcium (0.13% by weight, 0.04% by atomic percentage).

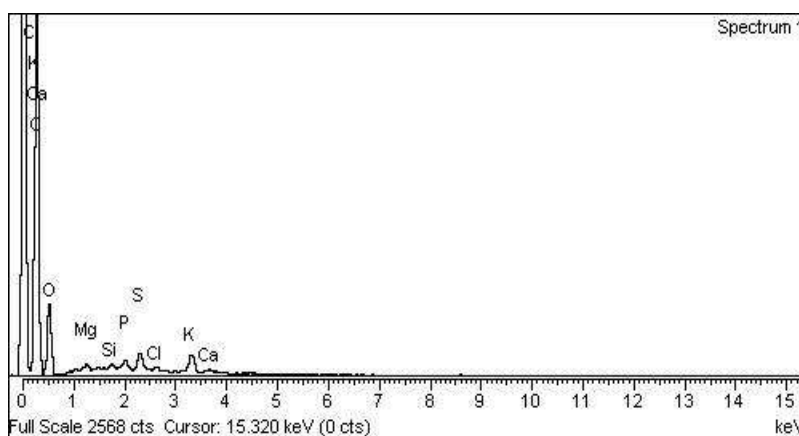


Fig. 3.5 The EDX analysis spectrum of *D. mucronata*.

IV. DISCUSSION

4.1 Antibacterial Activity

Microbial resistance an emerging threat to the humans although several antibiotics are also available in market that help in controlling bacteria but the infectious microbes developed resistance to that available antibiotics. The pre-existing antibiotics also have many side effects, toxicity, high cost, low solubility and also the negated discovery of new antibiotics over three decade create the requirement of novel sources for the antibiotics. Therefore, effective, secure and novel therapeutic agents with wide spectrum antibacterial compositions of high interest is vital (Behzad et al., 2021). Medicinal plants have significant role over years for their therapeutic properties against different microbes especially gram-negative bacteria. The therapeutical potential of these medicinal plants are due to presence secondary metabolites (phenol, saponin etc). Antimicrobial activities were carried out for the purpose of new source. The current studies of *D. mucronata* extracts reported the significant inhibition against selected bacterial and fungal strains. The results agree with the findings of (Zakaria-Nabti et al., 2020) that reported significant antibacterial Activity of Essential Oils from *Origanum glandulosum* Desf. against multidrug-resistant uropathogenic *K. pneumoniae*. (Salazar et al., 2018) reported the antibacterial activity of essential oil of *Baccharis dracunculifolia* DC (Asteraceae). The results revealed significant inhibition against *K. pneumoniae* and *E. coli* which confirmed similarity with the present results. Similarly, the result also supported by the results of (Jaafreh et al., 2019) that reported significant antibacterial activity of *Centeurea damascena* methanolic extract against *K. pneumoniae*. *E. coli* is being used common strain and causing urinary tract infections is inhibited by *Fragaria vesca* L. Isolated flavonoids, alkaloids, and saponins reported by (Hussain et al., 2020) similar with present results.

4.2 Antifungal Activity

The resistance of fungi to the market available drugs increased the risk of life threatening diseases. Natural sources are basic approaches that used for the extraction of safe, effective and negated side effects antibiotics. Plants are one of the source of natural isolated antibiotics have bioactive compounds responsible for many biological activities including antifungal activity (Hassan and Ullah, 2019). Keeping in view the above facts, the antifungal activity was experimented for checking of inhibitory potential of *D. mucronata* against fungal pathogens. The findings of the present experiments were agreeing with results of (Budniak et al. 2021) reported significant antifungal activity of water extract of *Gentiana cruciata* against *Candida albicans* (ATCC 885-653). (Dègnon et al. 2019) reported the antifungal activity of *Cymbopogon citratus* Essential Oil against *Aspergillus species* which confirmed the genuineness of present results. Similarly, the results also supported with the findings of (Dahar & Rai 2019) reported the momentous antifungal activity of *Ailanthus* spp, *Quassia* spp. and *Simarouba* spp. stem, bark and leaves extracts against *C. albicans* and *A. niger*. Other scientist (Marrez et al. 2021; O Elansary et al. 2020; Singh 2018; Taha et al. 2019) reported antifungal activities of medicinal plants extract against different fungal strains including *C. albicans*, *Aspergillus species* and *Alternaria alternate* having similar results to the present findings and validate the results. In Nutshell, the *D. mucronata* extracts have meaningful fungicidal effects which can be further scrutinize for antibiotics in future.

4.3 Phytotoxic Activity

Medicinal plants and allelopathic plants have potential bioactive compounds that have inhibitory effects and must use for the extraction of natural herbicides. The knowledge and identification of these allelochemicals or bioactive

compounds will be achieving through phytotoxic activity (Shi & Adkins, 2018). The phytotoxic activity of *D. mucronata* extracts showed significant inhibition against different tested seed (*B. compestris*, and *D. carota*). The current study agree with the results of (Rob *et al.* 2020) that reported the phytotoxic activity of phytotoxic compounds from *Schumannianthus dichotomus* extracts against AlfaAlfa, Cress, Barnyard grass and Italian ryegrass. The results also supported by the findings of (López-González *et al.* 2020) that reported phytotoxicity of Phytotoxic Activity of Norharmane (Natural Compound) against *Zea mays*, *Triticum aestivum*, *Oryza sativa*, *Lactuca sativa* and weeds like *Amaranthus retroflexus*. (Jiang *et al.* 2020) carried out phytotoxic activity of allelochemicals (athujone and eucalyptol) from *Artemisia sieversiana* against the weeds like *Amaranthus retroflexus*, *Medicago sativa*, *Poa annua* and *Pennisetum alopecuroides*. The reported significant results from (Jiang *et al.* 2020) study showed similarity to the present study. Several other researchers (Boonmee *et al.* 2018; Ma *et al.* 2019; Parra Amin *et al.* 2021) reported phytotoxic activity of different plants against crops and weeds that also in favor of current findings. Hence, the *A. cotula* have significant allelopathic effects that should have utilized for herbicides extractions in future.

4.4 GCMS analysis

A technique is used to analyze these substances qualitative and quantitatively called Gas Chromatography and mass spectrometry. GC-MS analysis is the combination of gas chromatography and mass spectrometry that identify different phyto-compounds in test samples (Sermakkani & Thangapandian 2012). The separation and identification of semi-volatile and volatile bioactive compounds through the technique of GC-MS which shows the liability of medicinal plants (Joseph *et al.* 2016). The compounds were identified and confirmed from the Retention time (RT), Peak area (%), similarity index (SI), Relative Similarity Index (RSI) and probability percentage from the library with peak and Retention time of sample test chromatograph. The present results agrees with the findings of (Joseph *et al.* 2016) that reported several compounds including 1-Deoxy-d-mannitol from the GCMS analysis of *Syzygium jambos* L. (Sermakkani & Thangapandian 2012) investigated Hexadecanoic acid methyl ester, Hexadecanoic acid ethyl ester and 1,2- Benzenedicarboxylic acid diisooctyl ester from the Gas Chromatography and Mass Spectrometry analysis of *Cassia italica* leaf extract. Similar work of (Elaiyaraja & Chandramohan 2016) who reported Eicosanoic acid methyl ester and Hexadecanoic acid ethyl ester from *Indonesiella echioides* (L.) leaves using GC-MS analysis. Hexadecanoic acid ethyl ester and 9,12-Octadecadienoic acid investigated by (Ziada *et al.* 2014) from the volatile oil of *D. mucronata* which agrees with present findings and also confirmed the authenticity of the analysis. Several other researchers reported the compounds with their medicinal properties from different plants also confirmed the therapeutical potential of *D. mucronata*.

4.5 EDX Analysis

The Energy Dispersive X-ray analysis generated data that comprised by spectra showing corresponding peaks to the element that are the exact composition of analyzed sample. The spectra indicate the ionization energies and the ordinates indicates the counts which mean higher the counts will be the presence of maximum distribution of that element of the hit spectra. Similarly, EDX analysis also indicates the presence of elements qualitatively and quantitatively. The present study of *D. mucronata* focused the elemental detection of the plant. The present results agrees with the findings of (Suman et al., 2013) that reported EDX of silver nanoparticles of *Ammannia baccifera* aerial parts and the peaks confirmed the detection of oxygen (at 0.4 KeV and chlorine at 2.5 KeV. The detection of C at 0.3 KeV were reported by (Cruz et al., 2010) in EDX analysis of *Lippia citriodora* synthesized silver nanoparticles supported the results. The findings were also supported by (Wang et al., 2020) who investigated Na at 1.0-1.1 KeV and Ca 3.5-3.8 KeV in the EDX analysis of silver nanoclusters of green tea extracts. (Rehana et al., 2017) analyzed EDX spectra of S at 2.3-2.5 KeV and K at 3.3-3.7 KeV of synthesized CuO nanoparticles of medicinal plants extracts, which testified the present results. Similarly, Mg at 1.2-1.4 KeV, Si at 1.6-1.9 KeV and P at 1.9-2.2 KeV of EDX spectra was reported by (Vijayakumar et al., 2013) that agrees with present findings. Investigated the Fe at 0.4-0.6, 6.3-6.6, 7.1-7.2 Kev and Al at 1.4-1.6 KeV of the EDX analysis of synthesized Ginger nano clay. (Rehana et al., 2017) reported O (42.75%), Cl (4.06%), K (3.65%), Ca (0.11%), S (0.08%), and P (0.05) by weight percentage in the EDX analysis of synthesized ZnO nanoparticles of different plant extracts. The results supported by (Vijayakumar et al., 2013) findings of percentage weight of C (17.33%), Si (20.03%), Al (5.78%), Na (1.82%), Mg (0.98%) and Fe (2.47%) of the EDX analysis of synthesized Ginger nano clay. Other researcher works also supported our results on basis of qualitative and quantitative (weight and atomic%) of elemental composition.

V. CONCLUSION

In conclusion, the study investigated the various fractions of *D. mucronata* for their antibacterial, antifungal, and phytotoxic activities. The N-hexane fraction exhibited significant antibacterial activity against *K. pneumonia*, *E. carotovora*, *X. vesicatoria*, and *Clavibacter michiganensis*, with the most potent effects observed at a concentration of 18µg/ml. The chloroform fraction also displayed remarkable antibacterial potential against the same bacterial strains, with the highest inhibition seen at 18µg/ml. Similarly, the ethyl acetate fraction demonstrated dose-dependent antibacterial activity against all tested strains, with the most substantial inhibition observed against *K. pneumonia*. In the case of antifungal activity, the N-hexane fraction showed varying effects on *C. albicans* and *A. Niger*, with the response depending on the concentration. Conversely, the chloroform fraction exhibited dose-dependent antifungal activity against both fungi, with the highest inhibition observed at 18µg/ml. The ethyl acetate fraction displayed a more complex response, with different concentrations affecting the two fungal strains differently. Furthermore, the phytotoxicity study revealed that *D. mucronata* extracts had inhibitory effects on the growth of *Daucus carrota* and *Brassica campestris*, with higher concentrations leading to more

pronounced inhibition of plumule and radicle lengths in both plant species. Finally, the GC-MS analysis identified several compounds in the chloroform extracts of *D. mucronata*, including camphor, caryophyllene oxide, ar-tumerone, thujanone, terpinen-4-ol, hexahydrofarnesyl acetone, cyclohexyl methane, trans-1,2-dimethylcyclohexane, 2,2,3,4-Tetramethylpentane, and 2,3,3-Trimethyloctane. Additionally, the EDX analysis revealed the elemental composition of *D. mucronata*, with carbon and oxygen being the major elements, along with trace amounts of magnesium, silicon, phosphorus, sulfur, chlorine, potassium, and calcium. In summary, this comprehensive study sheds light on the bioactive properties of different fractions of *D. mucronata*, providing valuable insights into its potential pharmaceutical and agricultural applications. Further research is warranted to explore the specific mechanisms behind these activities and to isolate and characterize the active compounds responsible for these effects.

REFERENCES

- Arndt, J., K. Deboudt, A. Anderson, A. Blondel, S. Eliet, P. Flament, M. Fourmentin, R. Healy, V. Savary, and A. Setyan. 2016. Scanning electron microscopy-energy dispersive X-ray spectrometry (SEM-EDX) and aerosol time-of-flight mass spectrometry (ATOFMS) single particle analysis of metallurgy plant emissions. *Environmental Pollution*. 210: 9-17.
- Ashraf, I., M. Zubair, K. Rizwan, N. Rasool, M. Jamil, S.A. Khan, R.B. Tareen, V.U. Ahmad, A. Mahmood and M.J.C.C.J. Riaz, 2018. Chemical composition, antioxidant and antimicrobial potential of essential oils from different parts of *D. mucronata* royle. 12(1): 1-8.
- Behzad, F., S. M. Naghib, S. N. Tabatabaei, Y. Zare, and K. Y. Rhee. 2021. An overview of the plant-mediated green synthesis of noble metal nanoparticles for antibacterial applications. *Journal of Industrial and Engineering Chemistry*. 94: 92-104.
- Bhalodia, N. R., and V. Shukla. 2011. Antibacterial and antifungal activities from leaf extracts of *Cassia fistula* l.: An ethnomedicinal plant. *Journal of advanced pharmaceutical technology & research*. 2(2): 104.
- Boonmee, S., Iwasaki, A., Suenaga, K., & Kato-Noguchi, H. (2018). Evaluation of phytotoxic activity of leaf and stem extracts and identification of a phytotoxic substance from *Caesalpinia mimosoides* Lamk. *Theoretical and Experimental Plant Physiology*, 30(2), 129-139.
- Budniak, L., Slobodianiuk, L., Marchyshyn, S., Basaraba, R., & Banadyga, A. (2021). The antibacterial and antifungal activities of the extract of *Gentiana cruciata* L. herb. *PharmacologyOnLine*, 2, 188-197.
- Cruz, D., P. L. Falé, A. Mourato, P. D. Vaz, M. L. Serralheiro, and A. R. L. Lino. 2010. Preparation and physicochemical characterization of Ag nanoparticles biosynthesized by *Lippia citriodora* (Lemon Verbena). *Colloids and surfaces B: biointerfaces*. 81(1): 67-73.
- Dahar, D., & Rai, A. (2019). Screening of antimicrobial and antioxidant potentials of some medicinal plants from Simaroubaceae family. *Journal of pharmacognosy and phytochemistry*, 8(4), 2576-2579.

- Dègnon, R., Allagbé, A., Adjou, E., & Dahouenon-Ahoussi, E. (2019). Antifungal activities of *Cymbopogon citratus* essential oil against *Aspergillus* species isolated from fermented fish products of Southern Benin. *Journal of food quality and hazards control*, 6(2), 53-57.
- Elaiyaraja, A., & Chandramohan, G. 2016. Comparative phytochemical profile of *Indoneesiella echioides* (L.) Nees leaves using GC-MS. *Journal of pharmacognosy and phytochemistry*, 5: 158.
- Hussain, S. A., S. Ahmad, Z. A. Butt, K. U. Rehman, S. Ullah, and S. S. Khan. (2020). Flavonoids, alkaloids, and saponins as antimicrobial agents from *Fragaria vesca* L. *Pure and Applied Biology*. Vol. 10, Issue 3, pp761-769. In.
- Imatomi, M., P. Novaes, M. A. F. M. Miranda, and S. C. J. Gualtieri. 2015. Phytotoxic effects of aqueous leaf extracts of four Myrtaceae species on three weeds. *Acta Scientiarum. Agronomy*. 37(2): 241-248.
- Jaafreh, M., K. Khleifat, H. Qaralleh, and M. Al-limoun. 2019. Antibacterial and Antioxidant Activities of *Centeurea damascena* Methanolic Extract. arXiv preprint arXiv:1911.02243.
- Jiang, C.-Y., Zhou, S.-X., Toshmatov, Z., Mei, Y., Jin, G.-Z., Han, C.-X., . . . Shao, H. (2020). Chemical composition and phytotoxic activity of the essential oil of *Artemisia sieversiana* growing in Xinjiang, China. *Natural product research*, 1-6.
- Joseph, D. D.; Veerasamy, K., & Singaram, S. S. 2016. Identification of bioactive compounds by gas chromatography-mass spectrometry analysis of *Syzygium jambos* (L.) collected from Western Ghats region Coimbatore, Tamil Nadu. *Asian Journal of Pharmaceutical and Clinical Research*, 10: 364-369.
- Kara, U., G. Susoy, S. A. Issa, W. Elshami, N. Y. Yorgun, M. Abuzaid, E. Kavaz, and H. Tekin. 2020. Scanning electron microscopy (SEM), energy-dispersive X-ray (EDX) spectroscopy and nuclear radiation shielding properties of [α -Fe³⁺ O (OH)]-doped lithium borate glasses. *Applied Physics A*. 126(7): 1-14.
- Khan, A., M. S. Khan, F. Hadi, G. Saddiq, and A. N. Khan. 2021. Energy-Dispersive X-ray (EDX) fluorescence based analysis of heavy metals in marble powder, paddy soil and rice (*Oryza sativa* L.) with potential health risks in District Malakand, Khyber Pakhtunkhwa, Pakistan. *Environmental Pollutants and Bioavailability*. 33(1): 301-316.
- Li, Z., Li, Q., Wang, J., Feng, Y., & Shao, Q. (2020). Impacts of projected climate change on runoff in upper reach of Heihe River basin using climate elasticity method and GCMs. *Science of the total Environment*, 716, 137072.
- López-González, D., Ledo, D., Cabeiras-Freijanes, L., Verdeguer, M., Reigosa, M. J., & Sánchez-Moreiras, A. M. (2020). Phytotoxic activity of the natural compound norharmane on crops, weeds and model plants. *Plants*, 9(10), 1328.
- Ma, K.-L., Wei, W.-J., Li, H.-Y., Song, Q.-Y., Dong, S.-H., & Gao, K. (2019). Meroterpenoids with diverse ring systems and dioxolanone-type secondary metabolites from *Phyllosticta capitalensis* and their phytotoxic activity. *Tetrahedron*, 75(33), 4611-4619.
- Marrez, D. A., Sultan, Y. Y., Naguib, M. M., & Higazy, A. M. (2021). Antimicrobial Activity, Cytotoxicity and Chemical Constituents of the Freshwater Microalga *Oscillatoria princeps*.
- Mukherjee, P. K., S. Bahadur, S. K. Chaudhary, A. Kar, and K. Mukherjee. (2015). Quality related safety issue-evidence-based validation of herbal medicine farm to pharma. In *Evidence-Based Validation of Herbal Medicine* (pp. 1-28).

- Naron, D., F.-X. Collard, L. Tyhoda, and J. Görgens. 2017. Characterisation of lignins from different sources by appropriate analytical methods: Introducing thermogravimetric analysis-thermal desorption-gas chromatography-mass spectroscopy. *Industrial crops and products*. 101: 61-74.
- O Elansary, H., Szopa, A., Klimek-Szczykutowicz, M., Ekiert, H., Barakat, A. A., & A Al-Mana, F. (2020). Antiproliferative, antimicrobial, and antifungal activities of polyphenol extracts from *Ferocactus* species. *Processes*, 8(2), 138.
- Parra Amin, J. E., Cuca, L. E., & González-Coloma, A. (2021). Antifungal and phytotoxic activity of benzoic acid derivatives from inflorescences of *Piper cumanense*. *Natural product research*, 35(16), 2763-2771.
- Pinto, E., M.-J. Gonçalves, C. Cavaleiro, and L. Salgueiro. 2017. Antifungal activity of *Thapsia villosa* essential oil against *Candida*, *Cryptococcus*, *Malassezia*, *Aspergillus* and dermatophyte species. *Molecules*. 22(10): 1595.
- Rehana, D., D. Mahendiran, R. S. Kumar, and A. K. Rahiman. 2017a. Evaluation of antioxidant and anticancer activity of copper oxide nanoparticles synthesized using medicinally important plant extracts. *Biomedicine & Pharmacotherapy*. 89: 1067-1077.
- Rehana, D., D. Mahendiran, R. S. Kumar, and A. K. Rahiman. 2017b. In vitro antioxidant and antidiabetic activities of zinc oxide nanoparticles synthesized using different plant extracts. *Bioprocess and biosystems engineering*. 40(6): 943-957.
- Rob, M., Hossen, K., Iwasaki, A., Suenaga, K., & Kato-Noguchi, H. (2020). Phytotoxic activity and identification of phytotoxic substances from *Schumannianthus dichotomus*. *Plants*, 9(1), 102.
- Salazar, G. J. T., J. P. de Sousa, C. N. F. Lima, I. C. S. Lemos, A. R. P. da Silva, T. S. de Freitas, H. D. M. Coutinho, L. E. da Silva, W. do Amaral, and C. Deschamps. 2018. Phytochemical characterization of the *Baccharis dracunculifolia* DC (Asteraceae) essential oil and antibacterial activity evaluation. *Industrial crops and products*. 122: 591-595.
- Sermakkani, M., & Thangapandian, V. 2012. GC-MS analysis of *Cassia italica* leaf methanol extract. *Asian J Pharm Clin Res*, 5: 90-94.
- Shi, B., & Adkins, S. (2018). Relative phytotoxicity of parthenium weed (*Parthenium hysterophorus* L.) residues on the seedling growth of a range of Australian native and introduced species. *Crop and Pasture Science*, 69(8), 837-845.
- Singh, S. (2018). *Senna* (*Cassia angustifolia* Vahl.): recent advances in pharmacognosy and prospects of cultivation in India. *Bioved*, 29(2), 399-408.
- Suman, T., D. Elumalai, P. Kaleena, and S. R. Rajasree. 2013. GC-MS analysis of bioactive components and synthesis of silver nanoparticle using *Ammannia baccifera* aerial extract and its larvicidal activity against malaria and filariasis vectors. *Industrial crops and products*. 47: 239-245.
- Taha, A. S., Salem, M. Z., Abo Elgat, W. A., Ali, H. M., Hatamleh, A. A., & Abdel-Salam, E. M. (2019). Assessment of the impact of different treatments on the technological and antifungal properties of papyrus (*Cyperus papyrus* L.) Sheets. *Materials*, 12(4), 620.

- Vijayakumar, M., K. Priya, F. Nancy, A. Noorlidah, and A. Ahmed. 2013. Biosynthesis, characterisation and anti-bacterial effect of plant-mediated silver nanoparticles using *Artemisia nilagirica*. *Industrial crops and products*. 41: 235-240.
- Wang, T., F. Zhang, R. Zhao, C. Wang, K. Hu, Y. Sun, C. Politis, A. Shavandi, and L. Nie. 2020. Polyvinyl alcohol/sodium alginate hydrogels incorporated with silver nanoclusters via green tea extract for antibacterial applications. *Designed monomers and polymers*. 23(1): 118-133.
- Zaidi, A., S.M. Bukhari, F.A. Khan, T. Noor and N. Iqbal, 2015. Ethnobotanical, phytochemical and pharmacological aspects of *D. mucronata* (thymeleaceae). *Tropical Journal of Pharmaceutical Research*, 14(8): 1517-1523.
- Zakaria Nabti, L., F. Sahli, H. Laouar, A. Olowo-Okere, J. G. Nkuimi Wandjou, and F. Maggi. 2020. Chemical composition and antibacterial activity of essential oils from the Algerian endemic *Origanum glandulosum* Desf. against multidrug-resistant uropathogenic *E. coli* isolates. *Antibiotics*. 9(1): 29.
- Ziada, M. A.; El-Sherbeny, G., & Askar, M. 2014. Ecology and phytochemistry of stinking chamomile (*Anthemis cotula* L.) in Egypt. *Asian Journal of Plant Sciences*, 13: 156-163.